Evaluation of the Linear Viscoelastic Force for a Dynamic System (*m, c, k*) Excited with a Rotating Force

Polidor BRATU
Research Institute for Construction Equipment and Technology - ICECON S.A., 266 Pantelimon Ave, 021652 Bucharest, Romania, icecon@icecon.ro

Andrei BURUGA
„Dunărea de Jos" University of Galati, Str. Domnească no. 47, Galati, Romania, andrei.buraga@dmmc.utm.md

Oleg CHILARI
„Dunărea de Jos" University of Galati, Str. Domnească no. 47, Galati, Romania, killari69@mail.ru

Adrian Ion CIOCODEIU
Institute of Solid Mechanics, Str. Constantin Mille 15, sector 1, Bucharest, Romania, adrian.ciocodeiu@gmail.com

Ionel OPREA
Institute of Solid Mechanics, Str. Constantin Mille 15, sector 1, Bucharest, Romania, oprea_january24@yahoo.com

Abstract: - The paper presents the topic of the representation of the hysteretic loops raised on the basis of the variation of the linear viscoelastic force $Q(x) = c\dot{x} + kx$ depending on the variation of the instantaneous displacement $x = x(t)$ of the linear dynamic system *m, c, k* dynamically excited with a harmonic excitation force $F = F(t) = F_0 \sin\omega t$. The linear Voigt-Kelvin dynamic model is characterized by the mass m, the viscous amortization c and the elastic constant k, being driven by the harmonic force in the F_0 amplitude and the ω pulsation. The representation of the *Q - x* hysteretic loop is made by an ellipse both by numerical testing and by experimental testing.

In order to optimize the energy dissipation capacity in the dissipative element, linear with the amortization constant *c*, representations of the parameterized ellipse families are required. Thus, we have to keep in mind that in the technological processes activated by vibration, the physical and mechanical parameters of the processed material may be modified, for example *c, k*, as well as the ω pulsation of the dynamic excitation.

It emerges that an analytical and graphic evaluation is required in order to highlight the parametric changes on the dynamic response and of the dissipated energy.

Consequently, for some real cases of processing in industry and constructions, the values of the physical and mechanical parameters were chosen, as well as the modality of their variation so as to be able to illustrate, as realistically as possible, the dynamic behaviour of the linear elastic system *m, c, k* dynamically excited with the given harmonic force.

Keywords: - hysteretic loops, linear viscoelastic force, dynamic system

1. INTRODUCTION

For the *m, c, k* linear dynamic model we define the fraction of the critical amortization $\zeta = \frac{c}{2}\sqrt{km}$ and the harmonic excitation force with the $F_0 = m_0 r\omega^2$, where $m_0 r$ is the static moment of the dynamic unbalance system at rotation with ω angular velocity, the same as the excitation pulsation so that $F = F(t) = F_0 \sin\omega t$.

The main objective of this study is to represent the families of curves for the three significant regimes Ω <1 ante-resonance, Ω = 1 resonance and Ω>1 post-resonance, where $\Omega = \frac{\omega}{\omega_n}$, with $\omega_n = \sqrt{\frac{k}{m}}$ when the parameter of the elliptic curves family is, in turn, *k, c,* ω with discreet variations in accordance with the requirement of the vibration-activated technological process.

In this context, the significant ellipses, their remarkable points, as well as the distribution of the ellipse set with the intersection points for the representative panel of the parameterized family are analysed.

In this paper there will be used calculation and analytical relations developed both by the author of this paper as well as by other authors with the corresponding references to the bibliography.

The following notations will be used: own pulsation $\omega_n = \sqrt{\frac{k}{m}}$; relative pulsation $\Omega = \frac{\omega}{\omega_n}$ the angle of loss in the viscoelastic system (*c, k*) noted with $\delta = \frac{c\omega}{k} = 2\zeta\Omega$. The physical units used in the paper will be specified both for the dynamic excitation $F = F(t) = F_0 \sin \omega t = m_0 r \omega^2 \sin \omega t$, as well as for the (*m, c, k*) system where $m = 10^4$kg, $m_0 r = 5$ kgm, and the *c, k* measurement units are discreetly variable.

For each situation, there will be analysed and graphically displayed the $A(\omega)$ displacement amplitude according to the discrete variable *k* or *c* parameter as well as the hysteretic loops $Q - x$ and $F - x$ with their significant points and their specified directions for the dynamic regimes of ante-resonance with $\Omega < 1$, resonance with $\Omega = 1$ and post-resonance with $\Omega > 1$.

2. EVALUATION OF LINEAR VISCOELASTIC FORCE *Q(x)* IN DYNAMIC HARMONIC REGIME

The *m, c, k* dynamic model of the harmonic dynamic excitation test equipment by the force $F(t) = m_0 r \omega^2 \sin \omega t$, is represented in figure 1, where the reaction $Q(x, \dot{x})$ is displayed as a result of the viscoelastic system deformation (*c, k*) for the instantaneous displacement $x = x(t)$ and the instantaneous speed $\dot{x} = \dot{x}(t)$

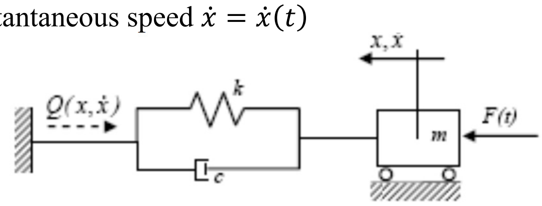

Figure 1. Dynamic diagram of the system (*m, c, k*)

The differential equation of motion is given as:

$$m\ddot{x} + c\dot{x} + k = F(t) \qquad (1)$$

with the solution $x = A \sin(\omega t - \varphi)$, where A is the amplitude of the displacement, and φ the phase shift between the instantaneous displacement x and the instantaneous force $F = F(t)$.

Force $Q(x, \dot{x})$ may be written down either as internal force according to *c, k*, either as reaction according to *F(t)* and $m\ddot{x}$, as follows:

$$Q(x, \dot{x}) = c\dot{x} + kx = F(t) - m\ddot{x} \qquad (2)$$

2.1. Linear viscoelastic force variance analysis *Q(x)*

For the dynamic test system *(m, c, k)* excited by the harmonic force *F (t)*, the significant parameters are the displacement amplitude $A = A(\omega)$ and the viscous-elastic reaction force $Q = Q(x)$ given by the relations:

$$A(\omega) = \frac{m_0 r \omega^2}{\sqrt{\left(k - m\omega^2\right)^2 + c^2\omega^2}} \qquad (3)$$

$$Q(x) = kx \pm c\omega\sqrt{A^2(\omega) - x^2} \qquad (4)$$

where $x = x(t)$ is the instantaneous displacement of the mass body *m*.

2.1.1. Variation of rigidity *k*

This study will be based on the following parametric values: $m = 10^4$ kg, $m_0 r = 5$kgm, $c = 5 \cdot 10^5$Ns/m, $\omega = 100$ rad/s and the discrete variation of *k* with the corresponding values for Ω as follows: $k_1 = 1/9 \cdot 10^8$ N/m, $\Omega_1 = 3$, $k_2 = 1/4 \cdot 10^8$ N/m, $\Omega_2 = 2$, $k_3 = 10^8$ N/m, $\Omega_3 = 1$, $k_4 = 2 \cdot 10^8$ N/m, $\Omega_4 = 0{,}7$, $k_5 = 4 \cdot 10^8$ N/m, $\Omega_5 = 0{,}5$.

The amplitude variation at the change of *k* and for $\omega = 100$ rad/s is A *(ω, k)* is represented in figure 2.

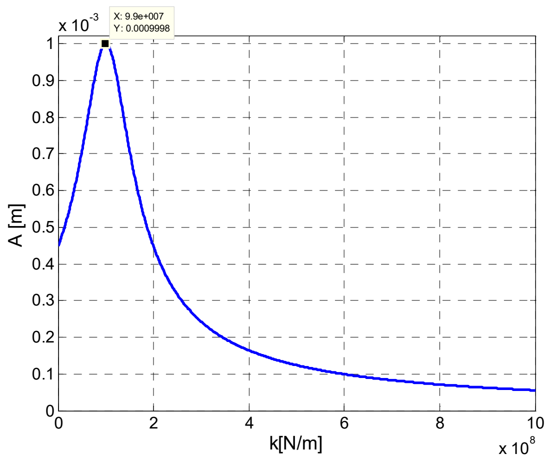

Figure 2. Variation of the amplitude according to $\omega = 100$ rad/s and for the continuous modification of k

For the hysteretic loops Q - x it is used relation (4) individualized by parameter k, as

$$Q(k,x) = kx \pm c\omega\sqrt{A^2(\omega,k) - x^2} \qquad (5)$$

which expresses the family of ellipses to the discrete variance of $k \in [k_1, \dots k_5]$ and the continuous variation of $x \in [-A(\omega,k), +A(\omega,k)]$. The graphical representation of the ellipse family is shown in figure 3. Table 1 shows the values of the ellipse areas values equivalent to the dissipated energy $W_d \equiv$ ellipse area expressed in J.

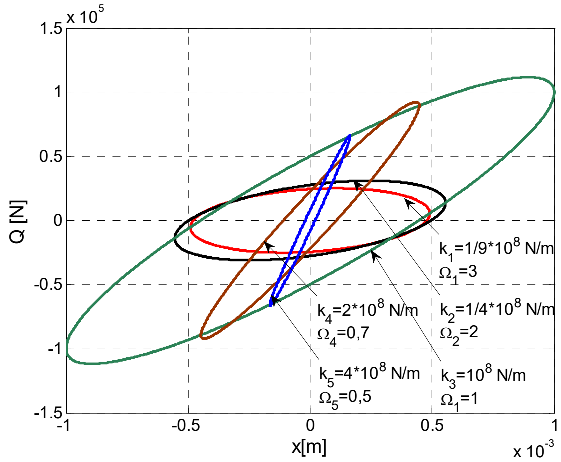

Figure 3 Family of ellipses Q - x

Table 1 shows that the maximum area of the ellipse of 157.07 corresponding to the maximum dissipated energy of 157.07 J for $\Omega = 1$ at resonance, as shown in figure 3 as well.

Table 1 Ellipses' areas for ω =100 rad/s

k[N/m] / Ω	$1/9 \cdot 10^8$	$1/4 \cdot 10^8$	10^8	$2 \cdot 10^8$	$4 \cdot 10^8$
3	37.75				
2		48.33			
1			157.07		
0,7				31.41	
0,5					4.24

It is noted that all ellipses, from Ω = 0.5 to Ω = 3, are inclined with the large axis only in trigonometric quadrant I.

2.1.2. Variation of viscous amortization c

The following parametric values will be used for the case study: $m = 10^4$ kg, $m_0 r$ = 5kgm, $k = 4 \cdot 10^5$N/m, ω = 100 rad/s. It emerges ω_n = 200 rad/s, Ω = 0,5. The variation of viscous amortisation c is obtained on the basis of the relation $c = 2\zeta\sqrt{km}$ and of the series of discrete values of the fraction from the critical amortisation ζ, as:. ζ_1=0.05, ζ_2=0.10, ζ_3=0.15, ζ_4=0.20, ζ_5=0.25. In this case the series of discrete values for c is as follows: $c_1 = 2 \cdot 10^5$Ns/m, $c_2 = 4 \cdot 10^5$Ns/m, $c_3 = 6 \cdot 10^5$Ns/m, $c_4 = 8 \cdot 10^5$Ns/m, $c_5 = 10 \cdot 10^5$Ns/m.

The variation of the amplitude A (ω, c) according to the continuous variation of c and the discrete value of ω = 100 rad/s is represented in Figure 4.

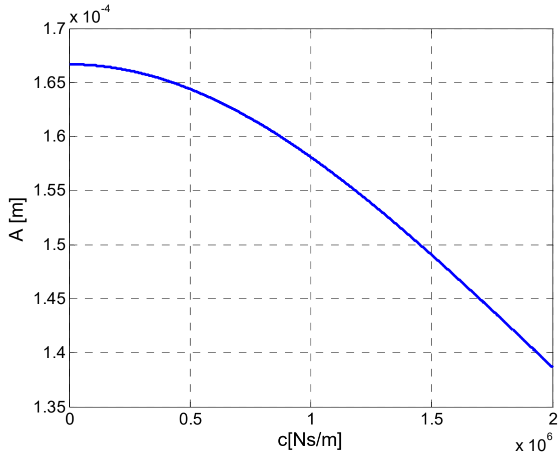

Figure 4 Variation of A according to the continuous modification of c, for ω = 100 rad/s

The hysteretic loops Q - x for the discrete variation of c, may be described based on relation (4), individualized by c, as follows:

$$Q(c,x) = kx \pm c\omega\sqrt{A^2(\omega,c) - x^2} \qquad (6)$$

which expresses the family of parameterized ellipses by the discrete variation of c and the continuous variation of $x \in [-A(\omega,c), +A(\omega,c)]$ represented in figure 5.

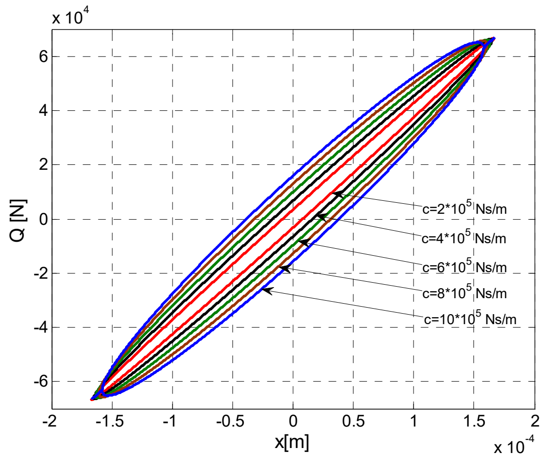

Figure 5 Family of ellipses with parameter c

Table 2 shows the values of o the ellipse areas with dissipated energies for the discrete values of c.

Table 2. Ellipses areas for ω =100 rad/s and Ω =0,5

c [Ns/m]	$2\cdot10^5$	$4\cdot10^5$	$6\cdot10^5$	$8\cdot10^5$	$10\cdot10^5$
area	1,73	3,4	5,03	6,51	7,85

2.1.3. Variation of the excitation pulsation ω

The case study for the dynamic model is characterized by system parameters as follows: $m = 10^4$ kg, m_0r = 5kgm, $k = 4 \cdot 10^5$N/m, $c = 5 \cdot 10^5$Ns/m, ω = 200 rad/s.

The discreet variation of the pulsation is given by the value string as follows: ω_1 = 100 rad/s, Ω_1 = 0,5, ω_2 = 150 rad/s, Ω_2 = 0,75, ω_3 = 200 rad/s, Ω_3 = 1, ω_4 = 300 rad/s, Ω_4 = 1,5, ω_5 = 400 rad/s, Ω_5 = 2.

Amplitude $A(\omega)$ is given by relation (3) for the continuous variation of pulsation ω and it is represented in figure 6.

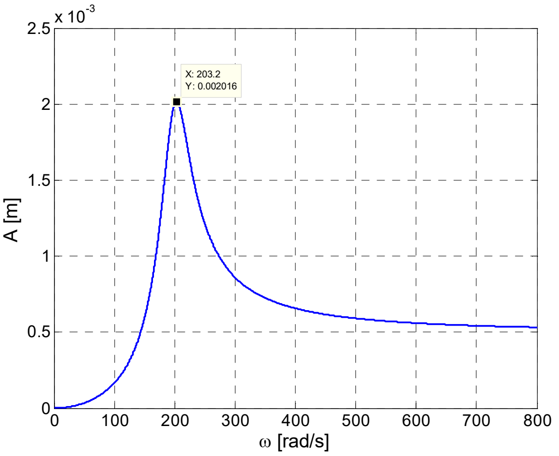

Figure 6. Variation of the amplitude according to the continuous modification of pulsation ω

The family of elliptical hysteretic loops is given by the parameter ω, based on relation (4), în according to ω, may be set as:

$$Q(\omega, x) = kx \pm c\omega\sqrt{A^2(\omega) - x^2} \qquad (7)$$

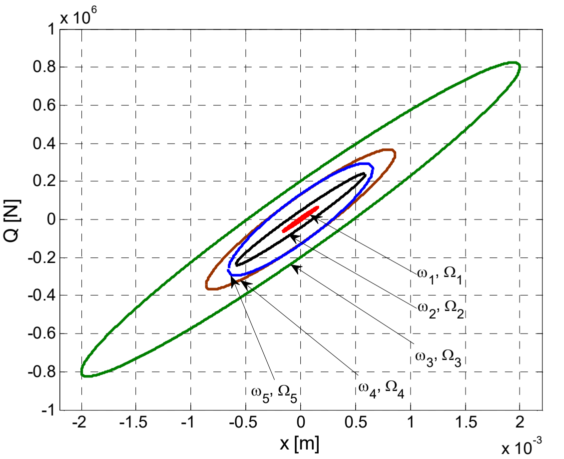

Figure 7. Family of elliptic hysteretic loops $Q - x$

with the discrete variance of ω and the continuous variation of $x \in [-A(\omega), +A(\omega)]$. The graphic representation is given in figure 7.

Table 3 shows the areas of the ellipses in figure 7, which corresponds to the energy dissipated per cycle for each individual pulsation from ω_1 = 100 rad/s to ω_5 = 400 rad/s.

Table 3. Ellipses' areas

Ω	0,5	0,75	1	1,5	2
ω, rad/s	100	150	200	300	400
area	4.24	82.26	1256.6	350.19	271.71

It is found that for Ω = 1, at resonance, the ellipse has the largest area and hence the maximum dissipated energy. In this case, the resonance ellipse circumscribes all ellipses in ante-resonance $\Omega < 1$ and post-resonance $\Omega > 1$. Also, all ellipses are inclined in the trigonometric quadrant I.

2.1.4. Specific parameters of the hysteretic elliptic loop $Q - x$

The remarkable points for the Q - x ellipse correspond to the intersection of the ellipse with the coordinate axes, the maximum values of force $Q(x)$ and the tangent points of the ellipse with straight lines parallel to the coordinate axes. Significant parametric values are also the angles formed by the significant straight or tangent lines to the elliptical loop in relation to the axes of the reference system Q - x.

Figure 8 shows the hysteretic elliptical loop for $\Omega > 1$, where all the remarkable points and characteristic angles are represented. The evaluation was made for the following measuring points: $m = 10^4$ kg, m_0r = 5kgm, $k = 4 \cdot 10^5$N/m, $c = 5 \cdot 10^5$Ns/m, ω = 300 rad/s, ω_n = 200 rad/s, Ω = 1,5, $c = 5 \cdot 10^5$Ns/m.

a) Coordinates of the remarkable points B, C, M, I

Point B corresponds to Q when $Q_B = 0$, and based on relation (4) it emerges

$$x_B = \pm A\frac{\delta}{\sqrt{1+\delta^2}} \qquad (8)$$

Point C corresponds to the case when $x = x_c = 0$, and based on relation (4) we have

$$Q_c = Q(0) = \pm c\omega A = \pm kA\delta \qquad (9)$$

Point M corresponds to the case of the maximum value of Q, that is for $Q' = \dfrac{dQ}{dt} = 0$ or

$$Q' = k \mp c\omega \frac{x}{\sqrt{A^2 - x^2}}$$, from where $x_M = \pm A \frac{1}{\sqrt{1+\delta^2}}$

where $\delta = \frac{c\omega}{k}$. Thus, the maximum force emerges as

$$Q(x_M, \omega) = Q_M^{\max} = \pm kA\sqrt{1+\delta^2} \qquad (10)$$

for

$$x_M = \pm A \frac{1}{\sqrt{1+\delta^2}} \qquad (11)$$

Point I correspond to the vertical tangent for $x = x_I = \pm A$, from where it emerges

$$Q_I = \pm kA \qquad (12)$$

that is the maximum elastic force, with the specification that the linear elastic force $Q(x) = \pm kx$.

b) ***The angular characteristics of the tangents to the ellipse in the remarkable points.***

Tangent to the ellipse in point B emerges for $x = x_B$ from the condition

$$Q'(x_B, \omega) = Q'_B = \left.\frac{dQ}{dt}\right|_{x_B} = k\left(1+\delta^2\right)$$

or

$$Q'(x_B, \omega) = tg\beta = k\left(1+\delta^2\right) \qquad (13)$$

Tangent to the ellipse in point C shall be obtained for $x = x_C = 0$ from the condition

$$Q'_C(0, \omega) = Q'_C = \left.\frac{dQ}{dt}\right|_{x=0} = k$$

or

$$Q'_C(0, \omega) = tg\alpha = k \qquad (14)$$

Tangent to the ellipse in point M, for $x = x_M = \pm A \frac{1}{\sqrt{1+\delta^2}}$ it is obtained the maximum value of Q as

$$Q_M^{\max} = Q_0 = \pm kA\sqrt{1+\delta^2} \qquad (15)$$

Tangent in point M is given by the relation

$$tg\gamma = Q'_M = k \mp c\omega \frac{x_M}{\sqrt{A^2 - x_M^2}} \qquad (16)$$

where by replacing $x_M = \pm A \frac{1}{\sqrt{1+\delta^2}}$, we obtain $tg\gamma = 0$, with $\gamma = 0$.

Tangent in point I is given by the relation

$$tg\varepsilon = Q'_I = k \mp c\omega \frac{x_I}{\sqrt{A^2 - x_I^2}} \qquad (17)$$

where by replacing $x_I = \pm A$ it emerges

$$tg\varepsilon = \infty, \text{ with } \varepsilon = \frac{\pi}{2}. \qquad (18)$$

Figure 8 shows all the previously established parametric measures.

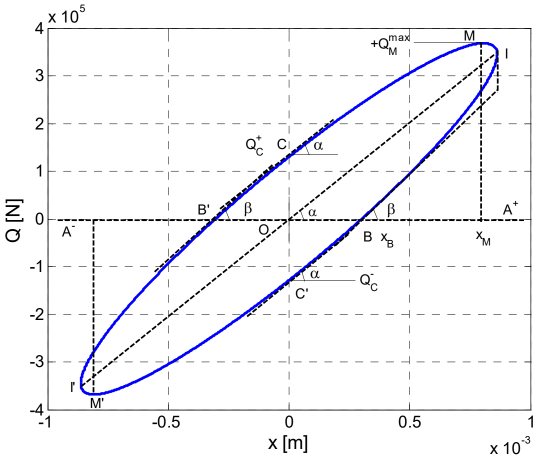

Figure 8. Hysteretic elliptic loop for **Ω >1**

2.2. Intersection of the hysteretic ellipses

The intersection points of two ellipses of the family of elliptical hysteretic loops are obtained for the condition $Q_i = Q_j$, where i is the value of the physical parameter of the ellipse of order i, and j is the discrete value of the same physical parameter p_j of the j order ellipse.

2.2.1. Family of ellipses with k parameter.

a) Dynamic regime in ante-resonance Ω<1

For two distinct values of the rigidity, that is at k_i and respectively k_j forces Q_i and Q_j have the following expresses

$$Q_i(\omega, k_i) = k_i x \pm c\omega\sqrt{A_i^2(k_i) - x^2} \qquad (19)$$

$$Q_j(\omega, k_j) = k_j x \pm c\omega\sqrt{A_j^2(k_j) - x^2} \qquad (20)$$

From the condition $Q_i(\omega, k_i) = Q_j(\omega, k_j)$ there emerge the abscissae x_{A1}, x'_{A1}, x_{A2} and x'_{A2}, with the ordinates corresponding to the forces, respectively Q_{A1}, Q'_{A1}, Q_{A2} and Q'_{A2}, represented in figure 9. The parametric values for which the two ellipses were raised are as follow: $m = 10^4$ kg, $m_0 r = 5$kgm, $c = 5 \cdot 10^5$Ns/m, $\omega = 100$ rad/s, $k_4 = 2 \cdot 10^8$ N/m, $\Omega_4 = 0{,}7$, $k_5 = 4 \cdot 10^8$ N/m, $\Omega_5 = 0{,}5$. In this case for points A_1, A'_1, A_2 and A'_2, it emerges:

$$A_1\begin{cases}x_{A_1}=7{,}7\cdot 10^{-5}m\\ Q_{A_1}=3{,}81\cdot 10^{4}N\end{cases};\quad A'_1\begin{cases}x_{A'_1}=-7{,}65\cdot 10^{-5}m\\ Q_{A'_1}=-3{,}77\cdot 10^{4}N\end{cases};$$

$$A_2\begin{cases}x_{A_2}=13{,}24\cdot 10^{-5}m\\ Q_{A_2}=4{,}8\cdot 10^{4}N\end{cases};\quad A'_2\begin{cases}x_{A'_2}=-13{,}12\cdot 10^{-5}m\\ Q_{A'_2}=-4{,}79\cdot 10^{4}N\end{cases}$$

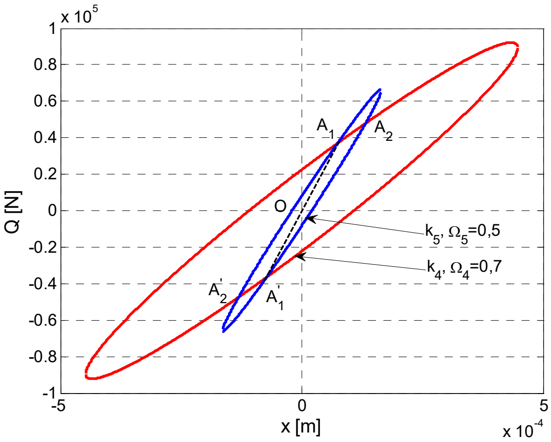

Figure 9. Intersection of ellipses k_4 and k_5 in ante-resonance

a) Dynamic regime in post-resonance $\Omega > 1$

The numerical values of the dynamic model for two ellipses parameterized by k_1 and k_2 are as follows: $m = 10^4$ kg, $m_0 r$ = 5kgm, $c = 5\cdot 10^5$Ns/m, $\omega = 100$ rad/s, $k_1 = 1/9\cdot 10^8$ N/m, $\Omega_1 = 3$, $k_2 = 1/4\cdot 10^8$ N/m, $\Omega_5 = 2$. In this case the intersection points of the two ellipses are P_1 , P'_1, P_2 and P'_2, with the following coordinates:

$$P_1\begin{cases}x_{P_1}=4{,}41\cdot 10^{-4}m\\ Q_{P_1}=-0{,}57\cdot 10^{4}N\end{cases};\quad P'_1\begin{cases}x_{P'_1}=4{,}38\cdot 10^{-4}m\\ Q_{P'_1}=0{,}60\cdot 10^{4}N\end{cases};$$

$$P_2\begin{cases}x_{P_2}=2{,}76\cdot 10^{-4}m\\ Q_{P_2}=-1{,}71\cdot 10^{4}N\end{cases};\quad P'_2\begin{cases}x_{P'_2}=2{,}80\cdot 10^{-4}m\\ Q_{P'_2}=1{,}68\cdot 10^{4}N\end{cases}$$

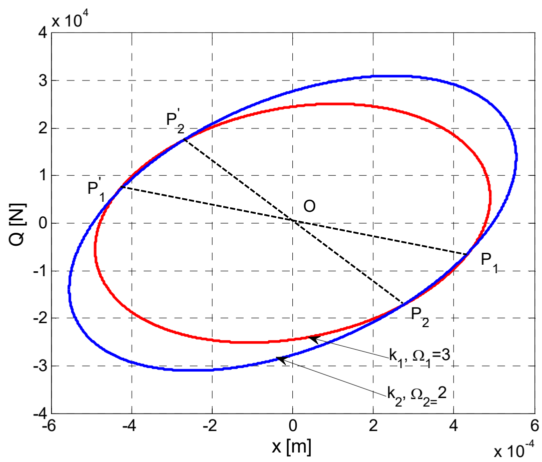

Figure 10. Intersection of the ellipses k_1 and k_2 in post-resonance

Figure 10 presents the intersection points of the ellipses k_1 and k_2 in post-resonance for $\Omega_1 = 3$ and respectively $\Omega_5 = 2$.

2.2.2. Family of ellipses with parameter *c*

For the case study we will use the parametric values of the dynamic system, as follows:
$m = 10^4$ kg, $m_0 r$ = 5kgm, $\omega = 100$ rad/s, $k = 2\cdot 10^8$ N/m, $\Omega = 0{,}7$; , $c_1 = 5\cdot 10^5$Ns/m, $c_2 = 10\cdot 10^5$Ns/m.

Forces Q_1 and Q_2 are given by the relations:

$$Q_1(c_1) = kx \pm c_1\omega\sqrt{A_1^2(c_1) - x^2} \tag{21}$$

$$Q_2(c_2) = kx \pm c_2\omega\sqrt{A_2^2(c_2) - x^2} \tag{22}$$

From the condition $Q_1(c_1) = Q_2(c_2)$ it emerges

$$x = x_H = \pm\sqrt{\frac{c_2^2 A_2^2 - c_1^2 A_1^2}{c_2^2 - c_1^2}} \tag{23}$$

where A_1 and A_2 are

$$A_1 = A_1(c_1) = \frac{m_0 r\omega^2}{\sqrt{\left(k - m\omega^2\right)^2 + c_1^2\omega^2}} \tag{24}$$

$$A_2 = A_2(c_2) = \frac{m_0 r\omega^2}{\sqrt{\left(k - m\omega^2\right)^2 + c_2^2\omega^2}} \tag{25}$$

Based on the relations (21)....(25) and on the previously established parametric values, we have the following coordinates for the intersection points:

$$H_1\begin{cases}x_{H_1}=3{,}16\cdot 10^{-4}m\\ Q_{H_1}=7{,}90\cdot 10^{4}N\end{cases};\quad H'_1\begin{cases}x_{H'_1}=-3{,}16\cdot 10^{-4}m\\ Q_{H'_1}=7{,}90\cdot 10^{4}N\end{cases};$$

$$H_2\begin{cases}x_{H_2}=3{,}16\cdot 10^{-4}m\\ Q_{H_2}=4{,}83\cdot 10^{4}N\end{cases};\quad H'_2\begin{cases}x_{H'_2}=-3{,}16\cdot 10^{-4}m\\ Q_{H'_2}=-4{,}85\cdot 10^{4}N\end{cases}$$

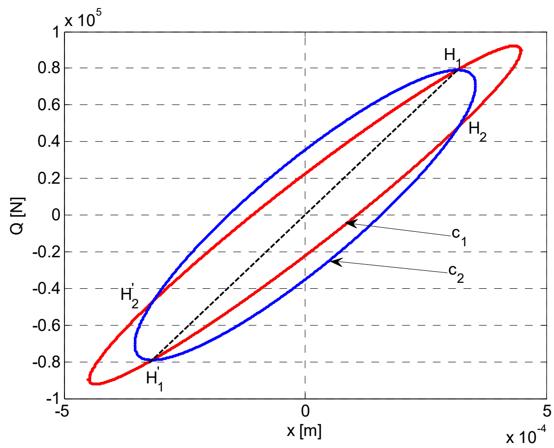

Figure 11. Intersection of the ellipses c_1 and c_2 for the ante-resonance regime $\Omega = 0.7$

Figure 11 presents the intersection points for ellipses c_1 and c_2.

2.2.3. Family of ellipses with parameter ω

The numeric values of the parameters of the dynamic model are: $m = 10^4$ kg, $m_0 r$ = 5kgm, $c = 5 \cdot 10^5$Ns/m, $k=10^8$ N/m ω_n = 100 rad/s, ω_1 = 200 rad/s, Ω_2= 2, ω_2 = 300 rad/s, Ω_2= 3. In this case forces Q_1 and Q_2 have the expressions:

$$Q_1(\omega_1) = kx \pm c\omega_1\sqrt{A_1^2(\omega_1) - x^2} \tag{26}$$

$$Q_2(\omega_2) = kx \pm c\omega_2\sqrt{A_2^2(\omega_2) - x^2} \tag{27}$$

with amplitudes A_1 and A_2 as

$$A_1 = A_1(\omega_1) = \frac{m_0 r\omega_1^2}{\sqrt{\left(m - k\omega_1^2\right)^2 + c^2\omega_1^2}} \tag{28}$$

$$A_2 = A_2(\omega_2) = \frac{m_0 r\omega_2^2}{\sqrt{\left(m - k\omega_2^2\right)^2 + c^2\omega_2^2}} \tag{29}$$

From the condition $Q_1(\omega_1) = Q_2(\omega_2)$ we obtain

$$x = x_R = \pm\sqrt{\frac{\omega_2^2 A_2^2 - \omega_1^2 A_1^2}{\omega_2^2 - \omega_1^2}} \tag{30}$$

Based on the relations (26)…(30) it emerges the coordinates of the intersection points R_1, R'_1, R_2 and R'_2, as follows :

$$R_1\begin{cases} x_{R_1} = 4{,}79 \cdot 10^{-5} m \\ Q_{R_1} = 9{,}08 \cdot 10^4 N \end{cases}; \quad R'_1\begin{cases} x_{R'_1} = -4{,}79 \cdot 10^{-5} m \\ Q_{R'_1} = -8{,}98 \cdot 10^4 N \end{cases};$$

$$R_2\begin{cases} x_{R_2} = 4{,}79 \cdot 10^{-5} m \\ Q_{R_2} = 0{,}63 \cdot 10^4 N \end{cases}; \quad R'_2\begin{cases} x_{R'_2} = -4{,}79 \cdot 10^{-5} m \\ Q_{R'_2} = -0{,}62 \cdot 10^4 N \end{cases}$$

Figure 12 shows ellipses ω_1 and ω_2 with the intersection points for the post-resonance regime.

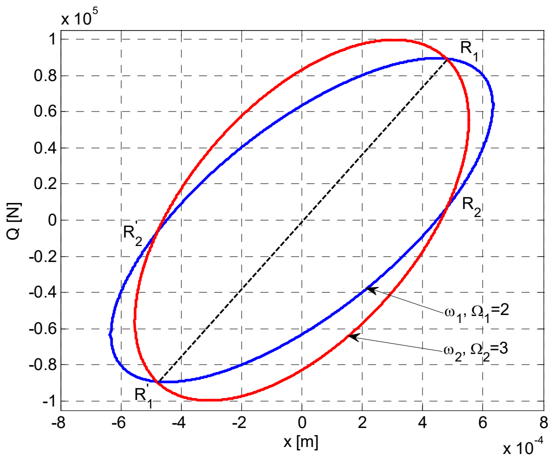

Figure 12. Intersection of ellipses $\omega_1$and ω_2 for the post-resonance regime

3. CONCLUSIONS

For a complete dynamic system (*m, c, k*) with linear Voigt-Kelvin viscoelastic connection with the dynamic harmonic excitation by force $F(t) = m_0 r\omega^2 \sin\omega t$, the parametric analysis of the dynamic response and of the hysteretic loop families, the following conclusions may be formulated:

a) the linear dynamic response in displacement is expressed by the amplitude *A* according to the continuous or discreet variation of the physical parameters *c, k* or of the kinematic excitation parameter ω, according to the graphical representations in figures 2, 4 and 6.

b) the families of hysteretic loops are characterized by the set of ellipses determined by physical parameters with discreet variation, in linear elastic and linear viscous regime. Thus, there were represented families of ellipses according to the physical parameters *k, c* and ω for dynamic regimes in ante-resonance $\Omega < 1$ or post-resonance $\Omega > 1$.

c) the ellipses' areas, being equal to the energy dissipated in the viscous linear element, constitute a significant criterion in the evaluation of the energy dissipation process for the dynamic harmonic system excited with force $F(t) = m_0 r\omega^2 \sin\omega t$.

d) the hysteretic loop of elliptical shape is analytically and graphically characterized based on the remarkable points and on the angles of the straight lines tangent to the ellipse in the points of physical significance.

e) the intersection points of the ellipses show that for some dynamic regimes, there may be identified remarkable individual properties of the system (*m, k, c*) excited by the harmonic force *F(t)*.

REFERENCES

[1] Dobrescu, C., *The rheological behaviour of stabilized bioactive soils during the vibration compaction process for road structures*, 22th International Congress on Sound and Vibration, Florence, Italy, 12-16.07.2015

[2] Forrest, James A., *Free-free dynamics of some vibration isolators*, Annual Conference of the Australian Acoustical Socyiety, 13-15 Nov. 2002, Adelaide, Australia

[3] Johnson, Erik A., Ramallo, Juan C., Spencer, Billie F. Jr, Sain, Michael K., *Intelligent base isolation systems*, 2nd World Conference on Structural Control, Kyoto, Japan, 1998

[4] Kim Young- Sang, *Study on the effective stiffness of base isolation system for reducing acceleration and displacement responses*, Journal of Korean Nuclear Society, vol.31, No. 6, pp. 586-594, Dec. 1999

[5] Kyu-Sik Park, Sang-Won Cho, In-Won Lee, *A comparative study on aseismic performances of base isolation systems for multi-span continuos bridge*, 14th KKNN Symposium on Civil Engineering, November 5-7, 2001, Kyoto, Japan

[6] Mitu, A.M., Sireteanu, T., Ghita, G., *Passive and Semi-Active Bracing Systems for Seismic Protection: A Comparative Study*, *Romanian Journal of Acoustics and Vibration,* Volume: 12 Issue: 1 Pages: 49-56, 2015

[7] Park, S. K., Han, K. B., *Effects of seismic isolation bearing with sliding mechanism on the response of brige*, Materials and Structures, vol.37, july 2004, pp 412-421

[8] Pinarbasi, Seval, Konstantinidis Dimitrios, Kelly, James M., *Seismic isolation for soft-story buildings*, 10th World Conference on seismic isolation, energy dissipation and active vibrations control of structures, Istanbul, Turkey, May 28-31, 2007

[9] Potirniche, A., *Assessments Regarding Effective Configurations of Vibration Isolators Based on Displacements Analysis*, Romanian Journal of Acoustics and Vibration, Volume: 12 Issue: 2 Pages: 126-131, 2015

[10] Sireteanu, T., *Smart Suspension Systems*, Romanian Journal of Acoustics and Vibration, Volume: 13 Issue: 1 Pages: 2-2, 2016

[11] Sireteanu, T., *The effect of structural degradation on the dynamic behaviour of buildings*, 9th WSEAS Int. Conf. on Acoustics & Music theory & Applications (AMTA '08), Bucharest, Romania, Jne 24-26, 2008

[12] Stanescu, N.D., *Vibrations of a Shell with Clearances, neo-Hookean Stiffness, and Harmonic Excitations*, *Romanian Journal of Acoustics and Vibration,* Volume: 13 Issue: 2 Pages: 104 -111, 2016

[13] Vasile, O., *Active Vibration Control for Viscoelastic Damping Systems under the Action of Inertial Forces*, *Romanian Journal of Acoustics and Vibration,* Volume: 14 Issue: 1 Pages: 54-58, 2017

[14] Wang, Yen-Po, *Fundamentals of seismic base isolation*, International training programs for seismic design of building structures hosted by National Certer of Research on Earthquake Engineering, Taiwan

[15] Xi-Yuan Zhou, Miao Han, Lin Yang, *Study on protection measures for seismic isolation rubber bearings*, ISET Jurnal of Earthquake Technology, Paper no.436, vol.40, no.2-4, June-December 2003, pp 137-160